

Final report

***Declining white satin moth activity on the east side of Lake Tahoe
varies across forest structure, leaf chemistry, and moisture gradients***

November 22, 2021

Prepared by:

Kellen Nelson, PhD

Research Forester

Pacific Northwest Research Station

USDA Forest Service

Sarah Bisbing, PhD

Assistant Professor

Department of Natural Resources & Environmental Science

University of Nevada-Reno

Chemical Ecology contributors:

Casey Philbin, PhD

Postdoctoral Scholar

Hitchcock Center for Chemical Ecology

University of Nevada-Reno

Lora Richards, PhD

Assistant Professor

Department of Biology

Hitchcock Center for Chemical Ecology

University of Nevada-Reno

Table of Contents

Table of Contents.....	1
Executive summary.....	2
Introduction.....	3
Methodology.....	4
Site selection	4
Aspen stand mapping	5
Field sampling.....	6
Stand inventories	6
Leaf sampling and chemical analysis	6
Data processing and analysis.....	8
Results.....	9
Aspen stand mapping	9
Aspen forests in the Carson Range.....	10
Extent and effects of white satin moth activity	14
Drivers of white satin moth occurrence and defoliation	18
Discussion.....	21
Implications for management	23
Acknowledgements.....	23
Literature cited	23
Appendix A: Supplementary material	26

Executive summary

Insect pest species cause extensive impacts to forest ecosystems each year resulting in forest production losses, extensive tree mortality, and consequences for ecosystem services. In the Lake Tahoe basin (California/Nevada, USA), populations of the non-native, invasive white satin moth (WSM, *Leucoma salicis*) have established in quaking aspen (*Populus tremuloides*) forests and have caused substantial defoliation for several years. In its larval stage, the WSM feeds on the leaves of *Salix* and *Populus* species, causing tree growth loss and dieback, especially after repeated defoliation events. Surprisingly, little research has investigated WSM ecology including the drivers of defoliation events. In this study, we investigated the patterns and drivers of WSM activity at tree, stand, and landscape scales to better understand factors that influence aspen stand susceptibility, the patterns of plant defensive compounds and their effect on WSM defoliation, and the extent of defoliation that has recently occurred across the Carson Range along the east side of the Lake Tahoe Basin, NV/CA, USA.

Aspen stand condition appears healthy across our plot network with abundant seedlings, saplings, and trees throughout the study region. Aspen abundances varied by size class and tree size distributions showed stands in varying phases of successional development. Impacts from WSM occurred in approximately half of stands throughout the Carson Range. Models predicting WSM presence in aspen stands indicated higher occurrence in stands with nearby WSM activity and greater basal area, and lower occurrence in stands with large conifers. Between 2018 and 2020, we observed broad declines in the proportion of trees affected and reductions in mean crown defoliation. The WSM showed a preference for larger aspen individuals and rates of infestation and defoliation declined more rapidly in smaller individuals as WSM activity declined. Models predicting the proportion of aspen affected by WSM showed strong positive associations with proximity to nearby WSM activity, basal area, and climatic moisture deficit.

Chemical compounds observed in aspen leaves across the Carson Range varied by tree life stage and across the study region. Differences in seedlings, saplings, and trees suggest that the suite of chemical compounds in leaves changes as aspen mature. Saplings exhibited a lower diversity of chemical compounds than trees, a pattern that is indicative that individuals in the sapling stage are investing more resources in growth over defensive chemistry. Chemical diversity also varied across the region and depending on the phase of stand development suggesting that environmental conditions and competition within stands may influence the expression of defensive compounds. Individual chemical compounds were strong drivers of WSM occurrence and percent crown defoliation in individual trees. Positive and negative associations were found indicating that some chemical compounds attract WSM herbivory while others are toxic or otherwise deter WSM herbivory. Leaf water content was negatively associated with tree crown defoliation further supporting our findings that WSM impacts decline with greater water availability.

Given the ample supply of suitable habitat, we expect the WSM to naturalize and expand further throughout the region. White satin moth activity is more pronounced on sites with water limitation and greater basal area; however, mixed aspen-conifer composition may lesser impacts. Stand improvement activities that promote host tree vigor, reduce competition, and provide protection from drought may mitigate growth impacts from defoliation, reduce the severity of defoliation, and/or facilitate recovery after periods of episodic population growth and decline. Greater resource availability improves the production of plant defensive chemical compounds.

Introduction

Insect pest species cause extensive impacts to forest ecosystems each year that can include forest production losses, extensive tree mortality, and consequences for ecosystem services and non-timber forest products industries such as tourism. Non-native invasive pests are no exception and can cause substantial impacts to host species as they establish and expand across native forests. In the Lake Tahoe basin (California/Nevada, USA), populations of the white satin moth (WSM, *Leucoma salicis*) have established in quaking aspen (*Populus tremuloides*) forests and recent population growth and expansion has caused substantial defoliation impacts for several years. Quaking aspen is renowned for its ecological, social, and economic value, and these values are particularly important in the iconic and heavily visited Lake Tahoe Basin. Surprisingly, little research has investigated WSM ecology, drivers of defoliation events, and the extent of impacts associated with a recent WSM outbreak in the Lake Tahoe Basin.

The WSM is a non-native, invasive defoliator belonging to the same family (Lymantriidae) as the infamous, non-native Gypsy moth (*Lymantria dispar*) that has defoliated North American deciduous tree species for over a century. In its larval stage, WSM feeds on the leaves of *Salix* and *Populus* species, causing tree growth loss and tree dieback, especially after repeated defoliation events. The species arrived from its native Eurasia origin in packing material and imported nursery stock in the 1910s and was first observed in British Columbia, Canada and near Boston, Massachusetts, USA (Burgess 1921). Since then, the WSM has spread along transportation corridors through 16 US states (USDS Forest Service 2019) and in Canada (Humphreys 1996). The WSM was identified as a significant land management issue in the Lake Tahoe Nevada State Park (LTNSP) management unit when localized aspen defoliation was first observed in 2012. Prior observations indicate that the WSM became established in other reaches of the Lake Tahoe Basin before 2012.

The WSM is aptly named after its white, fuzzy adult appearance that can be observed in mid-summer in deciduous host stands during mid-day and flying overhead in the morning and evenings. The life history of the WSM includes mating and egg laying in mid- to late-summer and maturation throughout the year in seven larval instars. After mating, eggs are laid on host leaves in bubbly masses that later dry into a hardened cake. Eggs hatch after approximately 14 days and larvae immediately begin feeding on late season deciduous host leaves. After leaf fall, second instar larvae overwinter in camouflaged hibernacula that can be found in cervices and on rough portions of host tree bark. Overwintering second instar larvae emerge in the late spring prior to leaf elongation and progress through the seventh instar feeding on early season host leaves. The greatest defoliation impacts occur in late-spring/early-summer when 7th instar larvae are approximately 10 cm long and appear black and hairy with distinct iridescent yellow and green patches on segments. Larvae pupate in a loosely woven silk cocoon and emerge as an adult moth after approximately 10 days. While the moth is capable of full flight, it is likely that longer-distance dissemination occurs via thermal updrafts, during wind events, and hitch-hiking on forest products and vehicles.

Upon introduction to a new area, the WSM establishes in nearby stands of host trees. Progressive dissemination and establishment of WSM in nearby stands is driven by factors that favor population growth such as weather conditions and the abundance of host tree forage in addition to landscape configuration and extent of host stands. Given the extent of naturalized populations in the USA (USDS Forest Service 2019), the WSM appears to be capable of

tolerating a wide range of environmental conditions. Periodic population irruption likely depends on conditions that favor reproduction and over-wintering success such as temperate seasonal temperatures and conditions that promote host tree vigor and early leaf emergence. Plant defense compounds are one way that host individuals can resist damage from defoliating insects, and multiple chemical compounds in quaking aspen have been found to negatively impact the growth, performance, and development of defoliator species (e.g., gypsy moth, aspen leaf miner (*Phyllocnistis populiella*), and western tent caterpillar (*Malacosoma californicum*); Hemming and Lindroth 2000, Young et al. 2010). Defensive compounds can vary negatively with aspen ramet age (Erwin et al. 2001, Donaldson et al. 2006) and height (Young et al. 2010), and positively in stands regenerating after disturbance such as burning (Erwin et al. 2001). Little is currently known about how white satin moth larvae and related defoliation may respond to plant defense compounds, nor how plant defense compounds vary within and among stands across the Lake Tahoe Basin.

As WSM expands across the Lake Tahoe Basin and into new locations across North America, understanding the effects of this emerging insect on host stands will be critical for land managers to respond appropriately to ongoing and upcoming outbreaks. Research on drivers and impacts of WSM defoliation on quaking aspen support management and conservation efforts to protect and promote quaking aspen locally and across its extensive range in North America. In this study, we investigate the patterns and drivers of WSM activity at tree, stand, and landscape scales to better understand factors that influence aspen stand susceptibility to WSM, patterns of plant defensive compounds and their effect on WSM defoliation, and the extent of defoliation that has recently occurred across the Carson Range along the east side of the Lake Tahoe Basin.

Methodology

Site selection

We assessed aspen stand structure and characterized patterns of WSM activity and defoliation in 62 aspen stands distributed across the Carson Range along the east side of the Lake Tahoe basin and in Dog Valley, CA (Figure 1). Sampling locations were determined using a spatially balanced, random sampling design across aspen forest types (Calveg vegetation cover dataset) and forest cover was confirmed via aerial imagery prior to visiting plots on the ground. Plots were established progressively each field season and remeasured for WSM defoliation activity in each subsequent year after plot establishment between 2018 and 2020. In 2018, 11 plots were established in North Canyon and around Marlette Lake in the Lake Tahoe Nevada State Park, Nevada. Plots in 2018 were arranged across a purported low to high white satin moth defoliation gradient. In 2019, 26 additional plots were established from Spooner Summit (US Highway 50) to Mount Rose Summit (NV-SR 431) and in Dog Valley, CA. In 2020, 8 additional plots were established from Spooner Summit to Mount Rose Summit and 17 plots were established south from Spooner Summit to Luther Pass.

Plots were grouped geographically into regions with a hierarchical cluster analysis using plot latitude and longitude data. Geographic names were assigned to groups of plots corresponding to the following regions: Dog Valley, Mount Rose – Slide Mountain, Hobart Reservoir, Marlette Lake – North Canyon, Genoa Peak, and Luther Pass (Figure 1).

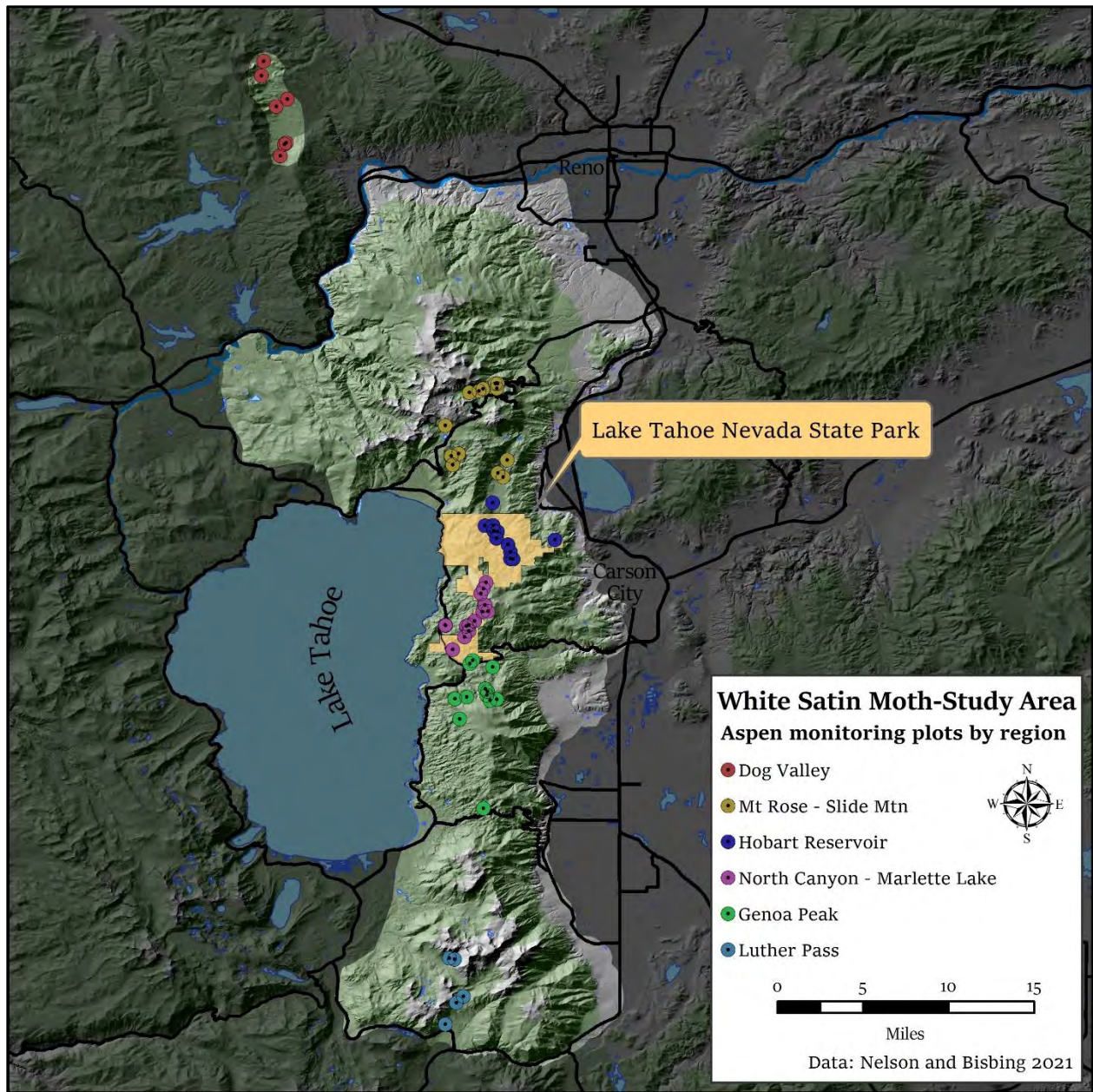


Figure 1: Map of plot locations by study area region in the Carson Range, NV/CA and Dog Valley, CA.

Aspen stand mapping

In 2020, we digitized aspen stands across several portions of the Carson Range on the east rim of Lake Tahoe to improve aspen stand delineation in our study region. We employed methods used by Tom Dilts (University of Nevada-Reno) that included digitizing aspen stands in Google Earth using historic imagery. To complement efforts by other recent investigators (Cushman and Dilts, personal communication, 2019/2020), our efforts were focused on the east side of the Carson Range crest from Galena Creek near Mount Rose to Luther Pass and Woodfords Canyon. These data were merged with a recent dataset developed by Tom Dilts for the Lake Tahoe Basin Management Unit (LTBMU) and several additional stands were delineated within the LTBMU. Delineated aspen stands were visually inspected for the presence or absence

of aspen during the 2020 field season; however, a rigorous evaluation of the map product was not conducted. Regardless, this new aspen stand map has proven to be a practical improvement over existing geospatial datasets. Aspen stands were rated with a confidence level to assist future map evaluation.

Field sampling

Stand inventories

At each plot location, we inventoried all seedlings (<1.37 m in height) and saplings (>1.37 m height and < 7.6 cm diameter) in a 0.02 ha fixed-radius circular plot (8 m radius) and trees (>7.6 cm diameter) were inventoried in a 0.1 ha circular fixed-radius plot (radius: 17.8 m) (Figure 2). Individuals were assessed for species, diameter at breast height (DBH; 1.37 m height, excluding seedlings), WSM occurrence, WSM defoliation damage, tree dieback, and mortality status (dead or alive). WSM occurrence was determined by inspecting trees for the presence of hibernacula, larvae, adult moth, cocoon, and egg masses. Defoliation was scored using the following scale: no herbivory – crown defoliation absent, light herbivory (<15% crown loss), moderate defoliation (15% to 90% crown loss), heavy defoliation (>90% crown loss), and dead (no sign of leafing out this season). To permit rapid remeasurement in subsequent years, we conducted intensive measurements of trees, sapling, and seedlings on N-S and E-W oriented transects (Figure 2). In each year, intensive measurements were made on 12 randomly selected seedlings, saplings, trees located at 5 m intervals radiating from plot center on transects. Height was additionally measured for all focal individuals. Intensive measurements were completed at peak defoliation during the month of July each year. Subsampling focal individuals in this way enabled remeasurement of an increasing number of plots each year during the period of peak defoliation while also establishing new plots to bolster our sample size and the inferences we were able to draw from the dataset.

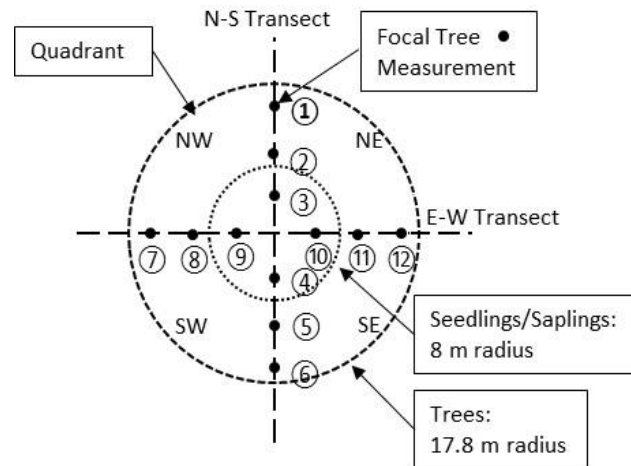


Figure 2: Forest inventory plot layout. Trees were inventoried within the 17.8 m radius fixed area plot and seedlings and saplings were inventoried within the inner 8.0 m radius fixed area plot. In 2019 and 2020, intensive measurements were collected on a subsample of focal trees at locations shown as solid dots.

Leaf sampling and chemical analysis

We collected leaf samples for chemical analysis in August 2019 and August 2020. In 2019, our objective was to compare chemistry across tree life stages and leaves were sampled from three seedlings, three saplings, and three trees across 8 plots in the North Canyon –

Marlette Lake and Hobart Reservoir regions (n=72). In 2020, our objective was to investigate landscape variation in leaf chemistry and leaves were sampled from two branches on each of three overstory trees across 27 plots and two branches were sampled from each of nine trees across two additional plots (n=198). Leaf collections in 2020 were taken across the Mount Rose – Slide Mountain, Hobart Reservoir, Marlette Lake – North Canyon, Genoa Peak, and Luther Pass regions of the Carson Range. Leaf collections from trees were taken at mid-crown using a pole pruner.

Leaf samples from each branch were divided into a fresh storage sample and a frozen storage sample. Fresh storage samples were kept on ice then refrigerated until being processed in the lab. Leaf area (WinFolia, Regent Instruments Inc., Canada), wet mass, and dry mass measurements were collected to compute leaf water content and specific leaf area. Frozen samples were placed on dry ice within 30 minutes of sampling, stored frozen at -80°C, and freeze dried for long-term storage and preparation for chemical analysis. Non-targeted metabolomics were adapted from methods previously described by Caseys et al. (2012). Three hole punched samples of five aspen leaves selected haphazardly from each branch were combined with a tungsten steel bead and ground in a tissue lyser (Quiagen Tissuelyser II) at 30 Hz for 3 min. Approximately 10.0 mg of ground leaf tissue were combined with 1.00 mL of HPLC grade methanol (Fisher, Waltham, MA) and briefly vortexed before 15 minutes of sonication. Samples were then centrifuged at 500 rpm (Genevac EZ-2) before filtering through 1 mL 96 well filter plates (glass fiber, 1 µm, Pall, New York, NY) into 1 mL 96 well plates and sealed with a silicone plate mat (Agilent, Santa Clara, CA). 100 µL aliquots of eleven samples from each row were combined to produce pooled samples, these pools were then combined in a similar fashion into a master pool of all samples. All samples (1 µL) were co-injected with a 1 µL air bubble and 1 µL of internal standard mix (ISD; salicylic acid-d₄, 0.480 mM; daidzin, 1.84 µM; daidzein, 2.56 µM in spectral grade MeOH, Fisher Optima). For quality control and to monitor instrument response, before the run and after every two rows of samples, ISD, master pool and an external standard mix (ESD; tremulacin, salicortin, salicin, salicylic acid, isoquercetin; rutin; trace amount used, diluted to above 10k count peak height) were injected. Between every two rows, pools of those two rows were co-injected with ISD for retention time alignment and structural determination. Analytical samples, pools and standards were injected onto an Agilent 1290 Infinity II UPLC equipped with a dual-channel variable wavelength detector ($\lambda = 254, 350 \text{ nm}$) connected to an Agilent 6560 ion-mobility-quadrupole-time-of-flight mass spectrometer equipped with a Jet Stream electrospray ionization dual source with reference mass infusion and tuned in 1700 *m/z* mode (IM-Q-TOF; drying gas temperature: 300 °C, drying gas flow: 11 L/m; drying gas flow: 11 L/m nebulizer pressure: 35 psig; sheath gas temperature: 300 °C; sheath gas flow: 10 L/m VCap: 3500 V; nozzle voltage: 0 V; fragmentor: 350 V; octopole: 750 V). All standards, analytical samples and pools were analyzed in TOF mode (1 scan per second) and standards and pools were also analyzed in iterative Auto Q-TOF mode (MS: 3 scans per second; MS/MS: 1 scan per second, collision energy: 20, 40 eV, precursor threshold: 8000 counts). Samples were eluted through an Agilent Poroshell 120 column (EC-C18, 1.9 µM, 2.1 x 100 mm) using a linear gradient comprised of solvent A (0.1 % aqueous formic acid) and solvent B (99% acetonitrile containing 1% water and 0.1 % formic acid) at 0.4 mL/min over 22 minutes as follows: 0 min: 1% B; 9 min: 20% B; 11 min: 50% B; 13-18 min: 100% B; 18.1-22 min: 1% B. Data were extracted and aligned using Agilent Profinder. Tandem mass spectrometry data were processed in Agilent Mass Hunter Qualitative Analysis. Putative structural annotations and chemical formulae were determined using high resolution molecular masses determined using

the Sirius 4 platform for determination of structural information (Dührkop et al. 2019), and where specific compounds are proposed, these were confirmed by comparison to experimental or *in silico* fragmentation patterns using CFM-ID and HMDB fragmentation spectral comparisons (Djoumbou-Feunang et al. 2019, Wishart et al. 2018). When fragmentation spectra could not confirm a putative compound assignment, chemical formulae and compound class were reported. Fragment-based phytochemical classification was carried out using CANOPUS (Dührkop et al. 2021) module within the Sirius 4 package.

Data processing and analysis

To investigate patterns in aspen forest structure across the Carson Range and prepare stand structure variables for modeling, we computed live and dead tree density, basal area, and quadratic mean diameter (QMD) and live seedling and sapling density for aspen and conifer species using tree measurement and count data from fixed area inventory plots. The proportion of trees affected by WSM and average WSM crown defoliation were computed using focal seedlings, sapling, and tree data for each year. The proximity to the nearest plot with WSM was computed as (1) the distance from each plot to the nearest WSM plot and (2) the average distance from each plot to the nearest three plots with WSM.

We assigned stands into representative structural groups by computing tree diameter distributions in each plot by binning stand density into 10 cm diameter bins for aspen and conifer species. Stand diameter distributions were grouped using a hierarchical cluster analysis and average diameter distributions were computed across all plots in each cluster group. Clustering was completed using Ward's method with a Bray-Curtis dissimilarity matrix and the optimal number of clusters was identified using the "elbow method".

We computed the diversity of chemical compounds found in aspen individuals by computing Shannon's diversity and inverse Simpson's diversity indices as composite variables for each sample tree. Shannon's method emphasizes richness and is weighted on rarer chemical compounds where the inverse Simpson's index emphasizes evenness and is weighted on more common chemical compounds.

We used analysis of variance (ANOVA), binomial logistic regression, and multiple pairwise comparisons (Tukey's HSD, $\alpha = 0.1$) to investigate how WSM activity, stand structure variables, and diversity of chemical compounds differed between regions and average diameter distribution groups. ANOVA was used for continuous variables and binomial logistic regression for proportion variables. Wilcoxon rank sum test was used in cases where data did not adhere to the assumption of a normal distribution. Change in the proportion of trees affected by WSM and mean crown proportion were computed by deducting annual plot estimates from prior year estimates. Whether or not change between years differed from zero was judged for statistical significance using Wilcoxon rank sum test.

We fit multivariate binomial generalized linear regression models (GLM) predicting WSM occurrence and proportion crown defoliation in trees to investigate how leaf characteristics and chemical compounds affect tree-level susceptibility to WSM. Binomial GLMs are a specific class of linear model appropriate for predicting binary (0,1) and proportional response variables. Specific leaf area, leaf water content, and hundreds of chemical compounds were evaluated as candidate predictors in the model using an exhaustive random forest model selection routine to minimize AIC. Predictor variables were scaled to permit comparison of coefficients. Assumptions for final models were confirmed using standard diagnostic plots, outliers were

identified for removal using Cook's distances, and the absence of multi-collinearity was confirmed by computing variance inflation factors.

We fit multivariate binomial generalized linear regression models predicting WSM occurrence and the proportion of aspen trees affected by WSM in stands to investigate how stand structure and environmental variables affect stand-level susceptibility to WSM. Models were fit by exhaustive model selection to minimize AIC using the following candidate predictor variables: stand structure (i.e., aspen density, aspen basal area, aspen QMD, conifer density, conifer basal area, conifer QMD), proximity to WSM (i.e., distance to the nearest white satin moth plot, average distance to the nearest three WSM plots), topography (i.e., elevation, heat load index, compound topographic index, topographic dissection), and historic climate variables (i.e., mean annual temperature, mean annual precipitation, mean annual radiation, mean May-to-September precipitation, precipitation as snow, climatic moisture deficit, and frost-free period). Topographic variables were computed using a digital elevation model via the ArcGIS 'Geomorphometry and Gradient Metrics Toolbox' tool (Evans et al. 2014) and historic climate variables (1981-2010) were extracted as scale-free point estimates using plot coordinates in ClimateNA v6.00 software (Wang et al. 2016). Predictor variables were scaled to permit comparison of coefficients. Sample plots in Dog Valley were excluded from the analysis because WSM was not found in the region. Assumptions for final models were confirmed using standard diagnostic plots, outliers were identified for removal using Cook's distances, and the absence of multi-collinearity was confirmed by computing variance inflation factors.

Data processing and statistics were conducted using the R software program (R Core Team 2019).

Results

Aspen stand mapping

We digitized approximate 636 aspen stands across portions of the Carson Range south of Mount Rose Wilderness (Figure 3). This resulted in a total of 888 distinct aspect stands when combined with 252 aspen stands digitized in other efforts along the Carson Range inside the Lake Tahoe Basin. Across all stands in the Carson range, average aspen stand size was 1.96 hectares and total area of aspen was estimated to be 1740 hectares. Mapping had not yet been conducted in the Mount Rose wilderness as of 2020.

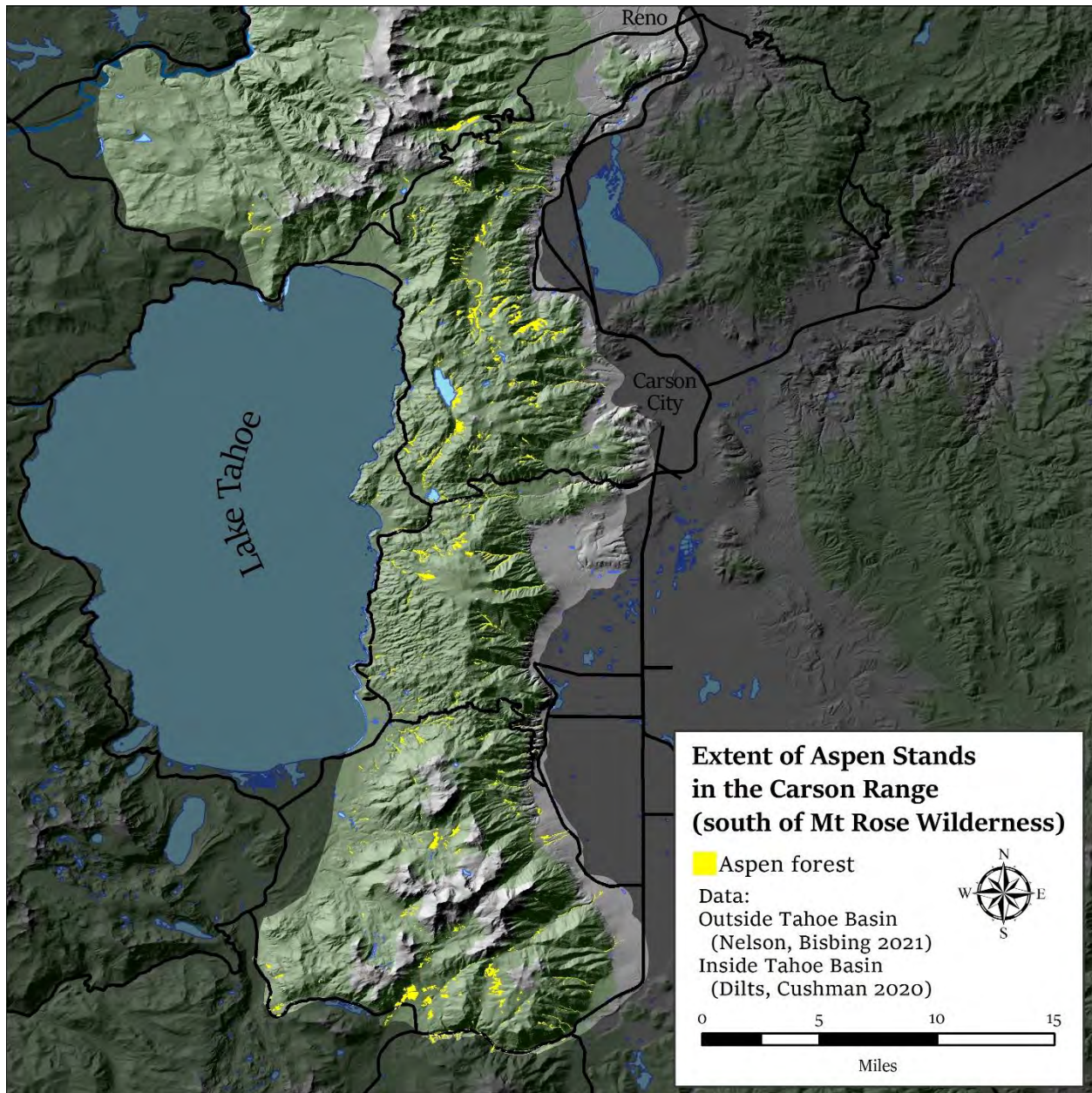


Figure 3: Extent of aspen stands in the Carson Range along east side of Lake Tahoe. Stands were mapped within the Lake Tahoe Basin by Cushman and Dilts (2020) and outside of the Lake Tahoe Basin by Nelson and Bisbing (2021 – this study).

Aspen forests in the Carson Range

We inventoried 9856 trees, 3940 saplings, and 6022 seedlings in 55 plots across the Carson Range along the east rim of Lake Tahoe and 7 plots in Dog Valley, CA. Plots in the Carson Range spanned 5 regions: Marlette Lake – North Canyon (n=14), Mount Rose – Slide Mountain (n=13), Genoa Peak (n=12), Hobart Reservoir (n=11), and Luther Pass (n=5). Ninety-five percent of plots contained greater than 50% aspen trees and 71% of plots contained greater than 90% aspen trees. See Appendix: Table 1 for a summary of species stand density.

Live aspen sapling and tree density and basal area did not differ significantly by study region, but live aspen QMD was found to be lower in Dog Valley than in other regions (Table 1). Aspen seedling density was greatest in the Marlette Lake – North Canyon region and lowest in Dog Valley but did not differ among other regions. Conifer sapling and tree density and QMD did not differ by region. Conifer basal area was greatest in Dog Valley but did not differ among other regions. Conifer seedling density was greatest in Dog Valley and lowest in the Mount Rose – Slide Mountain region but did not differ among other regions.

Table 1: Regional stand structure attributes. Means (\pm standard error) are reported for each attribute and letters denote statistical differences determined using Tukey’s HSD test ($\alpha=0.05$).

	Region						
	N. Canyon Marlette Lk	Mt Rose Slide Mtn	Genoa Peak	Hobart Reservoir	Luther Pass	Dog Valley	All Regions
Plots (n)	14	13	12	11	5	7	62
Aspen							
Seedlings (ha^{-1})	7730 \pm 1523 ^a	3382 \pm 445 ^b	4547 \pm 1130 ^{ab}	3341 \pm 909 ^b	3910 \pm 1000 ^{ab}	1826 \pm 717 ^b	4449 \pm 510
Saplings (ha^{-1})	3489 \pm 667 ^a	3941 \pm 736 ^a	2172 \pm 462 ^a	2551 \pm 793 ^a	4457 \pm 764 ^a	2004 \pm 743 ^a	3073 \pm 300
Trees (ha^{-1})	1260 \pm 134 ^a	1231 \pm 196 ^a	1123 \pm 175 ^a	1166 \pm 254 ^a	1328 \pm 293 ^a	1662 \pm 213 ^a	1262 \pm 82
Basal Area ($\text{m}^2 \text{ha}^{-1}$)	23.9 \pm 3.0 ^a	30.8 \pm 5.1 ^a	29.6 \pm 3.4 ^a	38.0 \pm 3.0 ^a	25.6 \pm 5.5 ^a	20.7 \pm 2.8 ^a	28.7 \pm 1.7
QMD (cm)	15.8 \pm 0.9 ^{ab}	18.9 \pm 2.6 ^{ab}	19.4 \pm 1.6 ^{ab}	23.3 \pm 2.1 ^a	17.8 \pm 4.2 ^{ab}	13.1 \pm 1.5 ^b	18.4 \pm 0.9
Conifers							
Seedlings (ha^{-1})	231 \pm 109 ^{ab}	42 \pm 29 ^a	228 \pm 94 ^{ab}	384 \pm 153 ^{ab}	10 \pm 10 ^{ab}	1840 \pm 1398 ^b	382 \pm 167
Saplings (ha^{-1})	36 \pm 16 ^a	46 \pm 24 ^a	217 \pm 143 ^a	127 \pm 46 ^a	30 \pm 20 ^a	75 \pm 33 ^a	91 \pm 29
Trees (ha^{-1})	96 \pm 40 ^a	136 \pm 49 ^a	141 \pm 54 ^a	181 \pm 49 ^a	48 \pm 21 ^a	142 \pm 43 ^a	129 \pm 20
Basal Area ($\text{m}^2 \text{ha}^{-1}$)	9.4 \pm 3.1 ^{ab}	7.2 \pm 1.7 ^a	6.6 \pm 1.9 ^a	7.5 \pm 2.1 ^a	1.8 \pm 0.8 ^a	22.7 \pm 8.6 ^b	8.9 \pm 1.5
QMD (cm)	25.2 \pm 5.9 ^a	29.0 \pm 5.5 ^a	20.7 \pm 3.4 ^a	20.4 \pm 3.2 ^a	18.9 \pm 9.3 ^a	37.5 \pm 7.9 ^a	25.2 \pm 2.3

Three dominant tree size distributions were identified using cluster analysis (Figure 4). The first distribution (1) exhibits a mounded distribution centered on sapling to pole size classes suggesting that canopy closure has occurred after a recent period of stand initiation. The second distribution (2) exhibits a significant conifer component spread across a gentle reverse-J distribution suggesting a self-sustaining multi-size stand condition with a moderate density of seedlings and small diameter trees and a substantial number of surviving large diameter trees. The third distribution (3) exhibits a sharp reverse-J distribution suggesting that these stands are undergoing stand re-initiation with high densities of suckers and saplings and low densities of large trees.

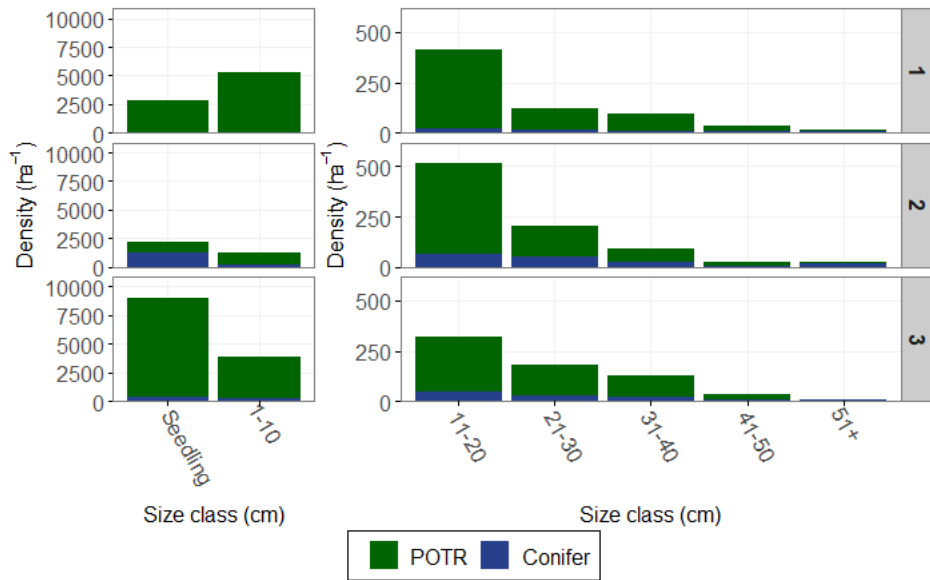


Figure 4: Dominant diameter distributions present in the Carson Range, NV. Note differing density scales in figure panels.

Our investigation of aspen leaf chemistry across the Carson range identified >500 unique chemical compounds with the 2019 and 2020 leaf datasets. Using the 2019 dataset, we found that the diversity of chemical compounds differed by aspen life stage with saplings exhibiting lower chemical diversity than trees (Figure 5). Seedlings chemical diversity did not differ from that of saplings or trees. In 2019, chemical diversity differed between the two sampling regions with seedlings, saplings, and trees in the North Canyon – Marlette lake region exhibiting greater chemical diversity than those in the Hobart Reservoir region (Figure 6).

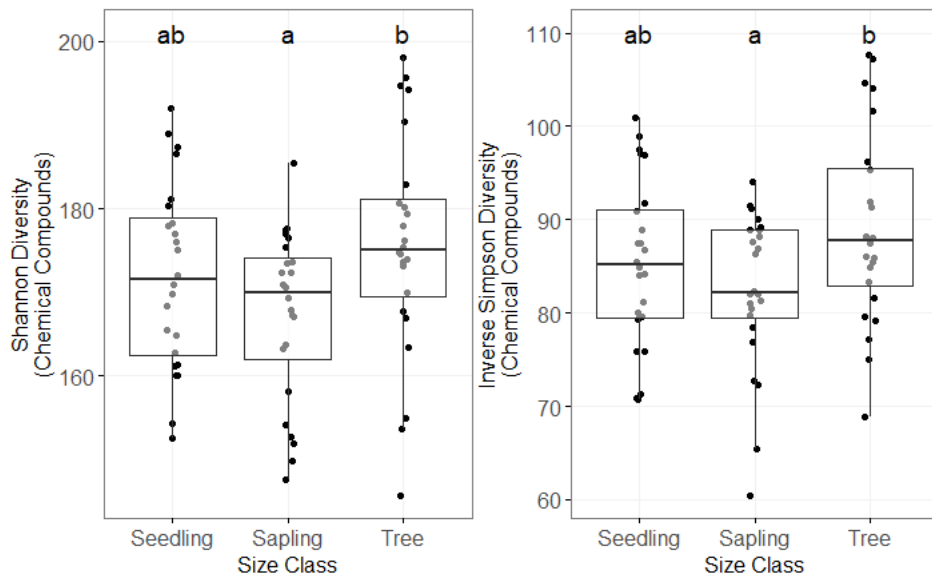


Figure 5: Shannon's diversity and inverse Simpson's diversity metrics computed from chemical compounds identified in seedling, sapling, and tree leaves collected across the Marlette Lake – North Canyon and Hobart Reservoir regions in 2019. Letters denote statistical differences between groups determined using Tukey's HSD test ($\alpha=0.05$).

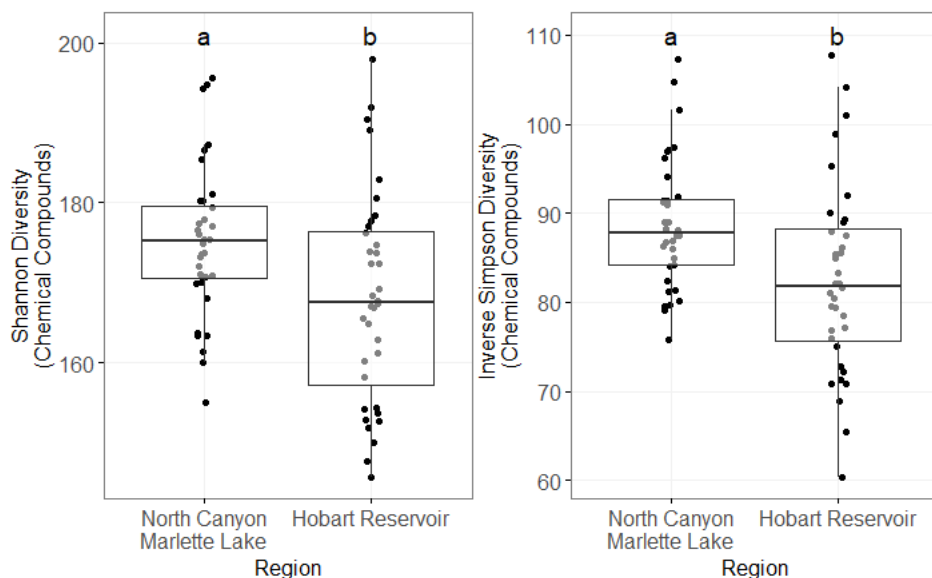


Figure 6: Shannon's diversity and inverse Simpson's diversity metrics computed from chemical compounds identified in seedling, sapling, and tree leaves collected across two study regions in 2019. Letters denote statistical differences between groups determined using Tukey's HSD test ($\alpha=0.05$).

The 2020 dataset collected across a broader set of stands in the Carson Range indicates that chemical diversity differs by region and in stands with differing tree size distributions. Aspen trees in the Mount Rose – Slide Mountain region had a lower diversity of chemical compounds but trees in other regions did not differ significantly in chemical diversity (Figure 7). We did not see a difference between trees in the North Canyon – Marlette Lake and Hobart Reservoir regions as was found in the 2019 data that included all tree life stages. In stands with differing tree size distributions, we found that chemical diversity is greatest in stands exhibiting self-sustaining multi-size structural traits and lowest in stands predominantly composed of sapling and small tree size classes (Figure 8). Trees in stands that exhibited structural characteristics of stand re-initiation including high densities of seedlings exhibited in intermediate level of chemical diversity and did not differ from stands with other size distributions.

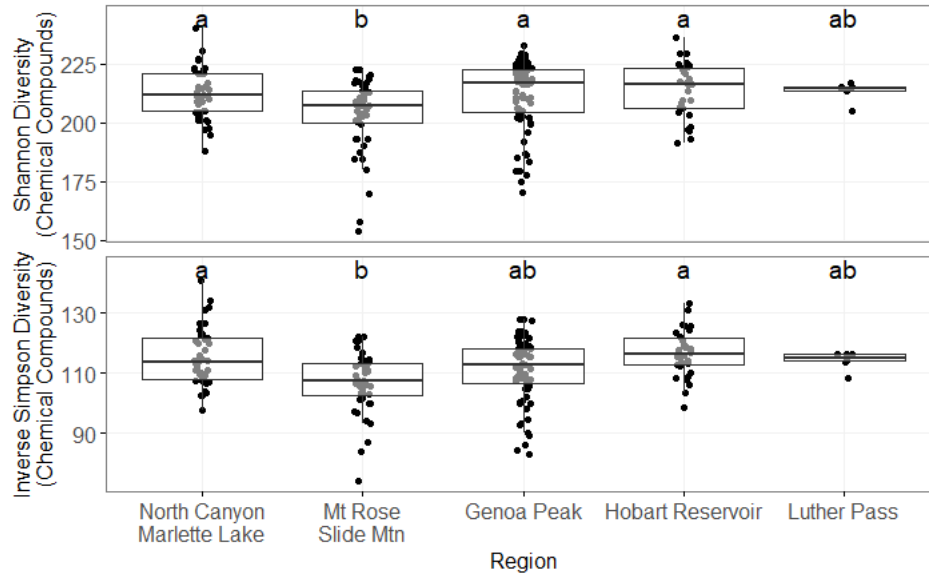


Figure 7: Shannon's diversity and inverse Simpson's diversity metrics computed from chemical compounds identified in leaves collected on trees in each study region in 2020. Letters denote statistical differences between groups determined using Tukey's HSD test ($\alpha=0.05$).

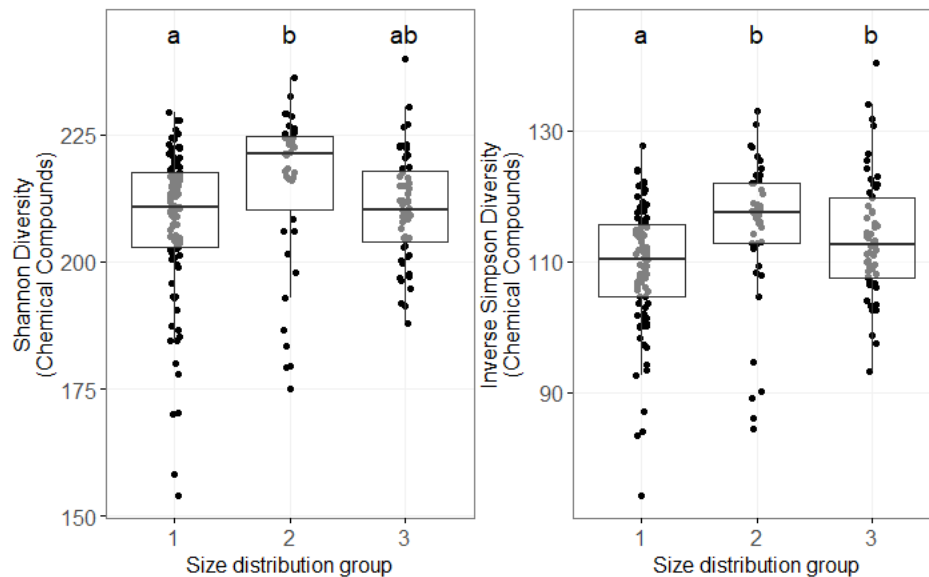


Figure 8: Shannon's diversity and inverse Simpson's diversity metrics computed from chemical compounds identified in leaves collected on trees in dominant tree size distribution groups in 2020. Letters denote statistical differences between groups determined using Tukey's HSD test ($\alpha=0.05$).

Extent and effects of white satin moth activity

We sampled an increasing number of plots each year across the Carson Range (Table 2). In 2018, WSM occurred in 8 out of 11 plots and had an average tree infestation rate of 92% in plots with WSM activity. In 2019, WSM occurred in 19 out of 37 plots and had an average tree infestation rate of 86% in plots with WSM activity. In 2020, WSM occurred in 29 out of 55 plots (Appendix: Figure 1) and had an average tree infestation rate of 63% in plots with WSM activity.

The number of plots recording WSM activity on seedlings and saplings was generally lower than the number of plots recording WSM activity on trees.

Table 2: Summary of WSM activity and impacts across our network of plots sampled in each year. Occurrence is presented as the number of plots with confirmed WSM activity and proportion of trees affected is reported as mean (± 1 standard error). Sample plots in Dog Valley were excluded because no WSM activity was observed in the region.

	Year		
	2018	2019	2020
Plots sampled (n)	11	37	55
Seedlings			
WSM occurrence [†]	-	16	8
Proportion affected [‡]	-	0.59 \pm 0.09	0.16 \pm 0.03
Saplings			
WSM occurrence [†]	-	19	23
Proportion affected [‡]	-	0.68 \pm 0.08	0.33 \pm 0.05
Trees			
WSM occurrence [†]	8	18	29
Proportion affected [‡]	0.92 \pm 0.07	0.86 \pm 0.07	0.63 \pm 0.06

[†]Reported as the number of plots with confirmed WSM activity.

[‡]Computed using plots with WSM activity only.

In the eleven plots established North Canyon – Marlette Lake region in 2018, the proportion of trees affected by WSM was very high across all plots in 2018 and 2019 but declined in 2020 (Figure 9). Mean WSM tree crown defoliation declined abruptly between 2018 and 2019 but did not change significantly between 2019 and 2020.

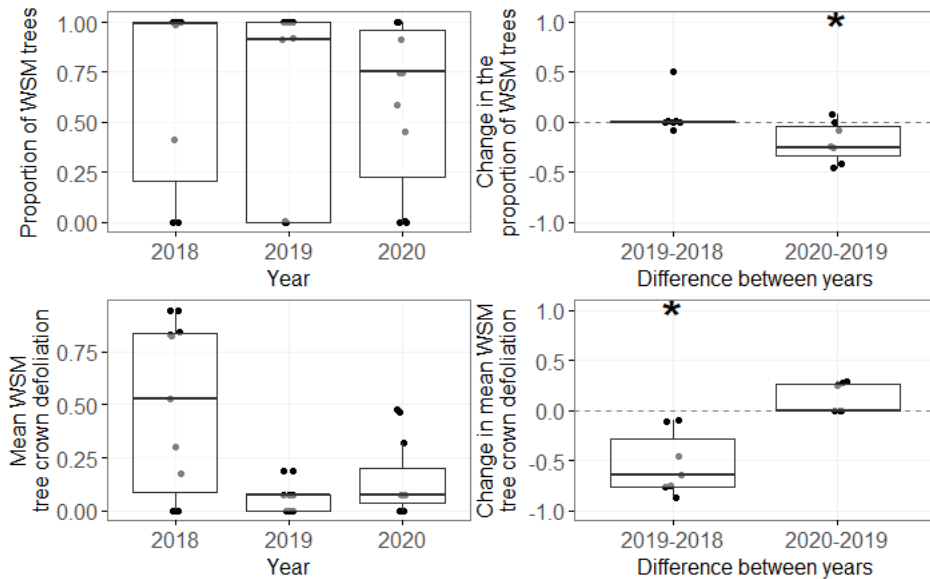


Figure 9: Change in the proportion of trees affected by WSM and change in mean tree crown WSM defoliation observed between sample years in North Canyon – Marlette Lake plots established in 2018. Only plots with WSM are shown (n=8). Asterisks denote statistically significant deviation from zero (no change) using Wilcoxon’s rank sum test ($\alpha < 0.05$).

In twenty-four plots monitored in 2019 and 2020 between US Highway 50 (Spooner Pass) to NV State Route 431 (Mount Rose Highway) with WSM activity, the proportion of

seedlings and saplings affected by WSM trees declined sharply between years, but trees did not show a significant change in the rate of infestation (Figure 10, Figure 11). Mean WSM seedling defoliation declined between 2019 and 2020, but mean sapling and tree WSM crown defoliation did not change between years.

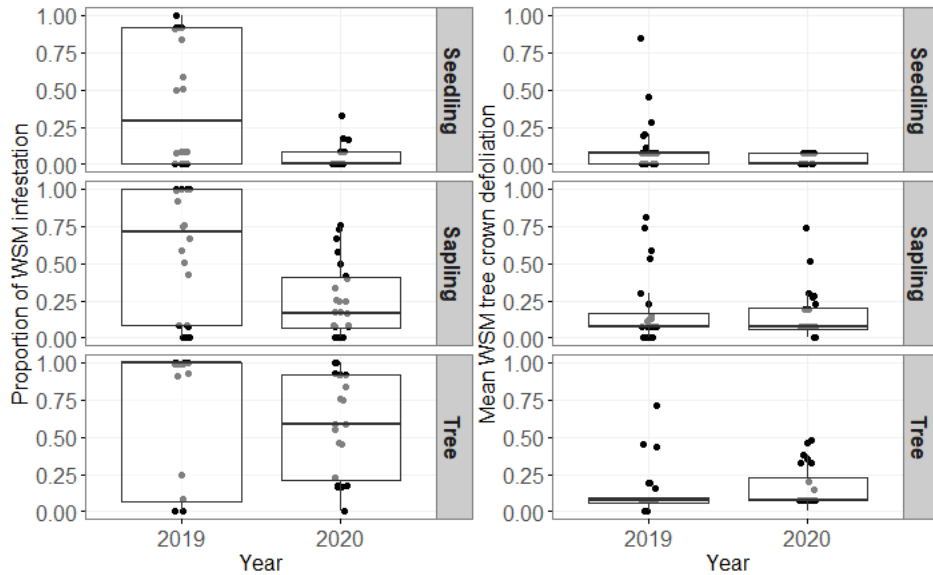


Figure 10: The proportion of seedlings, saplings, and trees affected by WSM and mean seedling, sapling, and tree crown WSM defoliation observed in 2019 and 2020. Plots were established across Marlette Lake – North Canyon, Hobart Reservoir, and Mount Rose – Slide mountain regions.

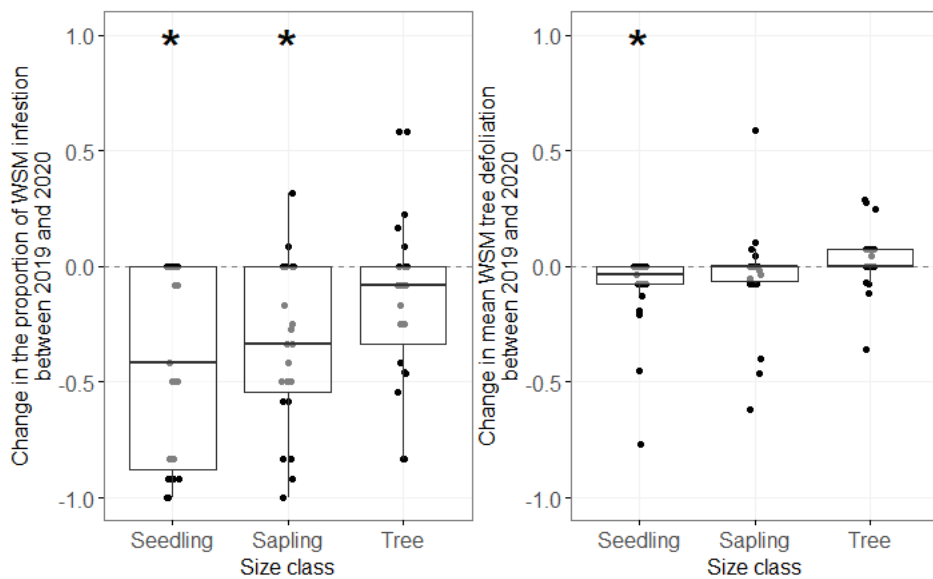


Figure 11: Change in the proportion of seedlings, saplings, and trees affected by WSM and change in mean seedling, sapling, and tree crown WSM defoliation observed between 2019 and 2020. Plots were established across Marlette Lake – North Canyon, Hobart Reservoir, and Mount Rose – Slide mountain regions. Asterisks denote statistically significant deviation from zero (no change) using Wilcoxon’s rank sum test ($\alpha < 0.05$).

The WSM occurred in plots spanning all regions sampled in the Carson Range but were not found in plots established in Dog Valley, CA (Table 3, Appendix: Figure 1). The greatest number of plots recorded WSM activity in the North Canyon – Marlette Lake and Hobart Reservoir regions. A lower number of plots with WSM were found in the Mount Rose – Slide Mountain region and only one infested plot was observed in the Luther Pass region. The proportion of individuals affected by WSM showed a rising trend in seedlings, saplings, and trees; however, the rate of WSM infestation did not differ statistically between regions within any single life stage.

Table 3: Regional summary of WSM activity and proportion of trees infested in 2020. Occurrence is presented as the number of plots with confirmed WSM activity and proportion of trees affected is reported as mean (\pm 1 standard error). Letters denote statistical differences between groups determined using binomial GLM regression and Tukey’s HSD test ($\alpha=0.05$).

Year = 2020	Region					
	Marlette Lk N. Canyon	Mt Rose Slide Mtn	Genoa Peak	Hobart Reservoir	Luther Pass	Dog Valley
Plots sampled (n)	14	13	12	11	5	7
Seedling						
WSM occurrence [†]	3	2	1	2	0	0
Proportion affected [‡]	0.19 \pm 0.07 ^a	0.02 \pm 0.01 ^a	0.25 ^a	0.08 \pm 0.00 ^a	-	-
Saplings						
WSM occurrence [†]	8	3	6	6	0	0
Proportion affected [‡]	0.26 \pm 0.05 ^a	0.47 \pm 0.20 ^a	0.28 \pm 0.11 ^a	0.40 \pm 0.11 ^a	-	-
Trees						
WSM occurrence [†]	9	3	7	9	1	0
Proportion affected [‡]	0.74 \pm 0.10 ^a	0.71 \pm 0.25 ^a	0.65 \pm 0.14 ^a	0.50 \pm 0.10 ^a	0.30 ^a	-

[†]Reported as the number of plots with confirmed WSM activity.

[‡]Computed using plots with WSM activity only.

The WSM exhibited similar effects on each dominant tree size distribution group (Figure 12). In stands that recently underwent re-initiation and had high abundances of sapling and pole size trees (size distribution 1), WSM occurred in 7 out of 22 plots and had an average tree infestation rate of 60% (Table 4). In stands that exhibited a self-sustaining multi-size distribution (size distribution 2), WSM occurred in 7 out of 12 plots and had an average tree infestation rate of 74%. Finally, in stands with the highest densities of seedlings and saplings, WSM occurred in 15 out of 21 plots and had an average tree infestation rate of 59%.

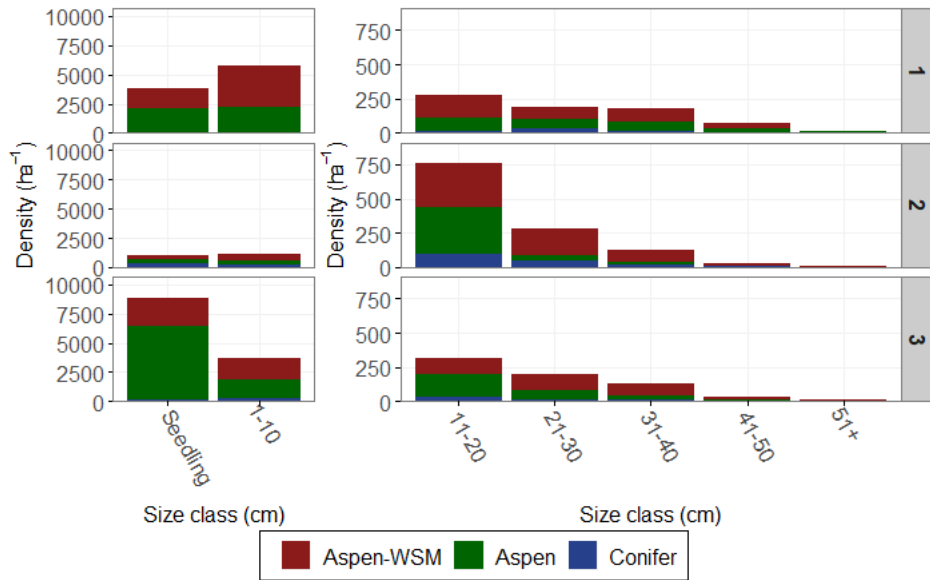


Figure 12: The number of trees affected by WSM in tree size distributions computed using stand inventory data collected in 2019 and 2020.

Table 4: Summary of WSM activity and proportion of trees infested in each dominant size distribution group in 2020. Occurrence is presented as the number of plots with confirmed WSM activity and proportion of trees affected is reported as mean (± 1 standard error). Letters denote statistical differences between groups determined using binomial GLM regression and Tukey's HSD test ($\alpha=0.05$).

Year = 2020	Dominant tree size distribution group		
	1	2	3
Plots sampled (n)	22	12	21
Seedlings			
WSM occurrence [†]	3	2	3
Proportion affected [‡]	0.17 \pm 0.08 ^a	0.21 \pm 0.04 ^a	0.11 \pm 0.03 ^a
Saplings			
WSM occurrence [†]	7	6	10
Proportion affected [‡]	0.31 \pm 0.11 ^a	0.49 \pm 0.10 ^a	0.25 \pm 0.04 ^a
Trees			
WSM occurrence [†]	7	7	15
Proportion affected [‡]	0.60 \pm 0.13 ^a	0.74 \pm 0.12 ^a	0.59 \pm 0.09 ^a

[†]Reported as the number of plots with confirmed WSM activity.

[‡]Computed using plots with WSM activity only.

Drivers of white satin moth occurrence and defoliation

Across all sample years, white satin moth activity disproportionately affected larger seedlings and trees (Table 5). The basal diameter of seedlings affected by WSM was greater than unaffected seedlings in 2019, but not in 2020 (at $\alpha < 0.05$ level). In 2020, WSM disproportionately affected seedlings of greater height; however, this was not observed in the 2019 data. In trees (individuals >1.37 m height), the WSM disproportionately affected individuals with larger diameters and heights in both 2019 and 2020.

Table 5: Comparison of seedling basal diameter and height and tree (>1.37 m height) dbh and height. Means (\pm standard error) are reported for individuals with and without signs of WSM defoliation. Differences were tested using Wilcoxon's rank sum test.

	WSM Lacking	WSM Present	W	p-value
Seedlings				
2019				
Height (m)	0.76 \pm 0.03	0.78 \pm 0.03	5924	0.519
Basal diameter (cm)	0.66 \pm 0.05	0.82 \pm 0.04	6931	0.004
2020				
Height (m)	0.79 \pm 0.02	0.97 \pm 0.08	2116	0.021
Basal diameter (cm)	1.1 \pm 0.04	1.29 \pm 0.14	1997	0.070
Trees				
2019				
Height (m)	7.5 \pm 0.5	9.3 \pm 0.4	53336	0.001
DBH (cm)	9.9 \pm 0.8	13.1 \pm 0.7	54206	<0.001
2020				
Height (m)	6.1 \pm 0.3	10.2 \pm 0.4	98404	<0.001
DBH (cm)	8.0 \pm 0.5	15.3 \pm 0.8	98821	<0.001

White satin moth occurrence and the proportion of crown defoliation in trees showed strong significant relationships with leaf chemistry (Table 6). The occurrence of the moth in individual trees was best predicted in a model exhibiting strong positive relationships with kaempferol (flavonoid glycoside), rutinoid (flavonoid glycoside), and traumatic acid (dicarboxylic acid/fatty acid) and strong negative relationships with choline (quaternary amine) and C₃₅H₂₈O₁₀ (phenolic glycoside). The proportion of crown defoliation in individual trees was positively associated with C₁₄H₂₀O₆ (phenolic glycoside) and traumatic acid (dicarboxylic acid/fatty acid) and negatively associated with C₂₈H₃₀O₁₄ (phenolic glycoside), C₃₅H₂₈O₁₀ (phenolic glycoside), and leaf water content (%). Chemical diversity metrics were not directly significant in regression models predicting WSM occurrence or crown defoliation in trees.

Table 6: Binomial GLM regression model results predicting tree WSM infestation (occurrence) tree crown defoliation (proportion) in trees with chemical compounds and leaf water content. Variables were scaled to enable comparison of coefficients.

Response	Variable	Coefficient	SE	Z	P	Pseudo-r ²	AIC
WSM occurrence in trees 2020 trees (df = 169)	Intercept	-0.001	0.303	-0.002	0.999	0.628	101.7
	Choline (quaternary amine)	-2.355	0.483	-4.87	<0.001		
	Kaempferol (flavonoid glycoside)	1.049	0.366	2.87	0.004		
	Rutinoside (flavonoid glycoside)	0.975	0.384	2.54	0.011		
	C ₃₅ H ₂₈ O ₁₀ (phenolic glycoside)	-2.537	0.527	-4.81	<0.001		
	Traumatic acid (dicarboxylic acid/fatty acid)	3.206	0.662	4.84	<0.001		
WSM tree crown defoliation 2020 trees (df = 177)	Intercept	-2.199	0.054	-40.95	<0.001	0.614	NA
	C ₂₈ H ₃₀ O ₁₄ (phenolic glycoside)	-0.179	0.058	-3.10	0.002		
	C ₁₄ H ₂₀ O ₆ (phenolic glycoside)	0.233	0.057	4.06	<0.001		
	Traumatic acid (dicarboxylic acid/fatty acid)	0.259	0.053	4.92	<0.001		
	C ₃₅ H ₂₈ O ₁₀ (phenolic glycoside)	-0.254	0.059	-4.29	<0.001		
	Leaf water content (%)	-0.420	0.054	-7.73	<0.001		

Binomial regression models predicting WSM occurrence in stands found that aspen basal area had a positive effect while distance to the nearest plot with WSM and conifer QMD had a negative effect on WSM occurrence (Table 7). Model coefficients were scaled such that the relative strength of each predictor variable might be evaluated. Scaled model coefficients indicate that distance to the nearest plot with WSM and aspen basal area had approximately twice the effect on WSM occurrence than conifer QMD.

Table 7: Binomial GLM regression model results predicting WSM infestation (occurrence) in aspen stands with environmental and stand structure variables. Variables were scaled to enable comparison of coefficients.

Year	Variable	Coefficient	SE	Z	P	Pseudo-r ²	AIC
All Years (df=52)	Intercept	-0.083	0.457	-0.18	0.855	0.529	42.115
	Distance to nearest WSM plot (km)	-2.632	0.922	-2.86	0.004		
	Aspen basal area (m ² ha ⁻¹)	2.152	0.696	3.09	0.002		
	Conifer QMD (cm)	-1.291	0.516	-2.50	0.012		

Binomial regression models predicting the proportion of aspen trees affected by WSM in stands found that distance to the nearest plot with WSM had a negative effect and aspen basal area and climatic moisture deficit had a positive effect on the rate of WSM infestation in stands (Table 8). Model selection was conducted independently for each year and identified the same predictor variables; however, differing infection rates in each year resulted in the 2019 model having greater explanatory power than the 2020 model (pseudo-r² = 0.67 in 2019 versus 0.59 in 2020). In both years' models, scaled model coefficients indicate that distance to the nearest plot with WSM has a 2-3 times greater effect on the proportion of trees affected than aspen basal area or climatic moisture deficit.

Table 8: Binomial GLM regression model results predicting the proportion of trees infested by WSM in aspen stands with environmental and stand structure variables. Variables were scaled to enable comparison of coefficients.

	Variable	Coefficient	SE	Z	P	Pseudo-r ²	AIC
2020 (df=50)	Intercept	-3.165	1.127	-2.81	0.005	0.593	37.075
	Distance to nearest WSM plot (km)	-5.424	2.115	-2.56	0.010		
	Aspen basal area (m ² ha ⁻¹)	2.209	0.792	2.79	0.005		
	Climatic moisture deficit (mm)	1.175	0.624	1.88	0.057		
2019 (df=34)	Intercept	-6.071	2.430	-2.50	0.013	0.671	23.761
	Distance to nearest WSM plot (km)	-12.115	4.727	-2.56	0.010		
	Aspen basal area (m ² ha ⁻¹)	4.589	1.935	2.37	0.018		
	Climatic moisture deficit (mm)	4.327	1.752	2.47	0.014		

Discussion

Aspen stand condition appears healthy across our plot network in the Carson Range, NV/CA with abundant seedlings, saplings, and trees throughout the study region. Aspen abundances varied by size class and size distribution and indicate stands in varying phases of successional development including stands currently undergoing re-initiation with high abundances of seedlings, stands that recently underwent re-initiation with high abundances of sapling and pole size trees, and self-sustaining stands with continuous recruitment. Conifer infilling appeared most prevalent in stands exhibiting self-sustaining size distributions with continuous recruitment. Re-initiation of stands in this study is likely tied to age related decline of decadent older cohorts that were not disturbed during the 20th century due to fire suppression or that arose after resource extraction activities in the 19th century (Rogers et al. 2007); however, we cannot rule out the possibility of sudden aspen decline and the cumulative effects of drought (Anderegg et al. 2012). Recent burning nor harvesting was present in the stands we investigated. Aspen stand structure did not differ across most study regions; however, seedling density as greatest in the North Canyon – Marlette Lake region and lowest in Dog Valley. Aspen size in terms of QMD was greatest in the Hobart Reservoir region and lowest in stands sampled in Dog Valley. Comparison of our data to other recent studies conducted in the Lake Tahoe region is difficult because other studies focused on large diameter tree classes and/or stands with a substantial conifer component; however, results from our plot network appear to show marginally higher densities, smaller average tree sizes, and lower conifer composition than other stands investigated at Lake Tahoe (Berrill et al. 2012, 2017). It is not surprising that stands sampled in this study have low proportions of conifers because our study design targeted stands believed to be pure aspen.

White satin moth impacts occurred in approximately half of stands we investigated and in each region of the study area (except Dog Valley). It is likely that WSM established along transportation corridors and readily spread to adjacent stands. Given the timing of introduction and ample supply of suitable habitat, we expect the WSM to naturalize and expand further throughout the region. Variation in the occurrence of WSM across regions is likely the result of time since introduction, the continuity of favorable host stands, and differences in climate regimes. Decline in the proportion of trees affected in each stand and reduction in the mean proportion of crown defoliation suggest insect populations declined between 2018 and 2020. Episodic population dynamics are common in Lepidoptera with population irruption occurring under conditions that improve reproductive rates such as periods of favorable seasonal weather and in stands with plentiful host forage. Population decline typically occurs within a couple of generations due to changes in seasonal weather (Ziennicka 2008), induction of plant chemical

defenses (Lindroth and St. Clair 2013), concomitant increases in predatory or parasitoid species that feed on irrupting populations, and/or high rates of disease spread in high density populations (Ziennicka 2008).

Chemical compounds observed in aspen leaves across the Carson Range were diverse and varied by tree life stage and more generally across the study region. Greater variation in Shannon diversity versus inverse Simpson diversity among individuals indicates greater variation in chemical compound richness with higher variation in rare minor compounds as opposed to variation in chemical compound evenness among major more common compounds. Differences in seedling, sapling, and tree life stages suggest that the suite of chemical compounds expressed changes as aspen mature. Saplings exhibited a lower level of richness and evenness of chemical compounds than trees, a pattern indicating that saplings are investing more resources in growth over defensive chemistry (Donaldson et al. 2006a, 2006b, Lindroth and St. Clair 2013). Across study regions, chemical compound richness and evenness was greater in the North Canyon – Marlette Lake region over the Hobart Reservoir region in 2019 and significantly lower in the Mt. Rose – Slide Mountain region than other regions in 2020. Such patterns are likely due to variation in environmental conditions across regions as has been demonstrated across elevation gradients in other areas (Pellissier et al. 2012). Across size distribution groups, trees found in self-sustaining stands with continuous recruitment had higher chemical compound richness over recently re-initiated stands dominated by saplings and pole size trees. Evenness in chemical compound diversity was greater in trees found in self-sustaining stands and in re-initiating stands with high seedling densities over recently re-initiated stands dominated by saplings and pole size trees. Competition within stands and variation in tree growth likely played a part in driving tree chemistry patterns found across tree size distributions.

Individual chemical compounds were strong drivers of WSM occurrence and percent crown defoliation in individual trees. Positive associations indicate compounds that attract WSM herbivory while negative associations indicate compounds that are toxic or otherwise deter WSM herbivory. In models predicting WSM occurrence in trees, rutinoid and kaempferol (flavonoid glycosides) and traumatic acid (a dicarboxylic acid/fatty acid) were indicated as attractants. Choline (a quaternary amine) and a phenolic glycoside were both strong deterrent compounds. In models predicting tree crown defoliation, traumatic acid and a phenolic glycoside were both indicated as attractants where two additional phenolic glycosides were indicated as deterrents, possibly as antifeedants. Traumatic acid is a phytohormone used to stimulate healing after leaf damage and while it is likely a response to leaf damage caused by herbivory, it may also serve as an aggregation signal for nearby moths. Choline is a precursor to neurotransmitters, membrane lipids and osmo-regulating molecules in plants and has been previously shown to increase in response to simulated herbivory in oak seedlings (Sardans et al. 2014). However, we observed that aspens with higher levels of choline were less likely to have WSM present, suggesting choline may have more direct anti-herbivore activity. Phenolic glycosides are a relatively broad class of compounds that are widely acknowledged as deterrents to herbivory in aspen and are associated with reduced feeding, growth, and survival of insect defoliators (Hemming et al. 2000, Lindroth and St. Clair 2013).

The probability of WSM presence in a stand and the rate of trees affected by WSM were both best predicted by the proximity of stands to nearby WSM activity and stand structure attributes indicative of the concentration of nutritionally optimal forage in a stand. The importance of nearby WSM populations indicates that WSM adheres to density and distance

dependent rules of population growth and dispersal. The presence of conifers in a stand decreases the density of host trees, requiring greater energy expenditure for the WSM to search for mates and forage. Beyond selecting stands with greater overall forage (i.e., aspen basal area), the WSM also exhibited a preference for trees of larger diameter and height, traits associated with greater leaf area. Finally, leaf water content was important in predicting tree crown defoliation and climatic moisture deficit was important in predicting rate of trees affected by WSM in stands. Both of these relationships align with the notion that WSM populations prosper and defoliation is heightened on sites with greater water limitation.

Implications for management

- Continued spread of the WSM is likely across the Carson Range due to the extent of suitable host habitat and because the insect is already widely distributed across the range. Establishment will occur more quickly in host stands that are in close proximity to stands already infested by WSM.
- Tree defoliation and the rate of WSM infestation are more pronounced on water limited sites. Drought years are likely to initiate population irruptions of WSM.
- Greater impacts from the WSM are likely in stands with higher basal area. Stands with mixed aspen-conifer composition may experience lesser impacts from the WSM.
- Stand improvement activities that promote host tree vigor, reduce competition, and provide protection from drought may mitigate growth impacts from defoliation, reduce the severity of defoliation, and/or facilitate recovery after periods of episodic population growth and decline. Greater resource availability improves the production of plant defensive chemical compounds.
- Understanding leaf chemical composition and the diversity of chemical compounds found in aspen stands across the Carson Range improves our ability to explain patterns of defoliation and herbivory.

Acknowledgements

We would like to thank Kelsey Glastetter, Alex Pitman, Tessa Putz, Maggie Shepherd, and Erica Sutherland for forestry field and laboratory support, and Jennifer McCracken for chemical ecology laboratory support. Thanks to Gene Phillips (Nevada Division of Forestry) for his help funding and designing this project. We would also like to acknowledge assistance from Mark Enders (Nevada Fish and Game), Roland Shaw (Nevada Division of Forestry) Anna Belle Monte (Humboldt-Toiyabe National Forest), and Duncan Leao (Humboldt-Toiyabe National Forest) for their deep regional knowledge and help finding sites with white satin moth. We also thank Mick Hitchcock for his generous endowment to fund the Hitchcock Center for Chemical Ecology and his donation to purchase the Agilent IM-Q-TOF instrumentation. Also, we thank Agilent Technologies for a grant to purchase the Agilent UPLC used in this study. Finally, we would like to thank Tom Dilts for his input on mapping aspen stands in the region and Alex Pitman for conducting the mapping.

Literature cited

Anderegg, W.R., Berry, J.A., Smith, D.D., Sperry, J.S., Anderegg, L.D. and Field, C.B., 2012. The roles of hydraulic and carbon stress in a widespread climate-induced forest die-off.

- Proceedings of the National Academy of Sciences, 109(1), pp.233-237.
<https://doi.org/10.1073/pnas.1107891109>.
- Berrill, J.P. and Dagley, C.M., 2012. Geographic patterns and stand variables influencing growth and vigor of *Populus tremuloides* in the Sierra Nevada (USA). *International Scholarly Research Notices*, 2012. <https://doi.org/10.5402/2012/271549>.
- Berrill, J.P., Dagley, C.M., Coppeto, S.A. and Gross, S.E., 2017. Curtailing succession: Removing conifers enhances understory light and growth of young aspen in mixed stands around Lake Tahoe, California and Nevada, USA. *Forest Ecology and Management*, 400, pp.511-522. <https://doi.org/10.1016/j.foreco.2017.06.001>.
- Burgess, A.F., 1921. The satin moth: an introduced enemy of poplars and willows (Vol. 167). US Department of Agriculture.
- Caseys, C., Glauser, G., Stölting, K.N., Christe, C., Albrechtsen, B.R. and Lexer, C., 2012. Effects of interspecific recombination on functional traits in trees revealed by metabolomics and genotyping-by-resequencing. *Plant Ecology & Diversity*, 5(4), pp.457-471.
<https://doi.org/10.1080/17550874.2012.748850>
- Davidson, C.B., Gottschalk, K.W. and Johnson, J.E. 1999. Tree mortality following defoliation by the European gypsy moth (*Lymantria dispar* L.) in the United States: a review. *Forest Science*, 45(1), pp.74-84. <https://doi.org/10.1093/forestscience/45.1.74>.
- Djombou-Feunang, Y., Pon, A., Karu, N., Zheng, J., Li, C., Arndt, D., Gautam, M., Allen, F. and Wishart, D.S., 2019. CFM-ID 3.0: significantly improved ESI-MS/MS prediction and compound identification. *Metabolites*, 9(4), p.72.
<https://doi.org/10.3390/metabo9040072>.
- Donaldson, J.R., Kruger, E.L. and Lindroth, R.L., 2006a. Competition-and resource-mediated tradeoffs between growth and defensive chemistry in trembling aspen (*Populus tremuloides*). *New Phytologist*, 169(3), pp.561-570. <https://doi.org/10.1111/j.1469-8137.2005.01613.x>.
- Donaldson, J.R., Stevens, M.T., Barnhill, H.R. and Lindroth, R.L., 2006b. Age-related shifts in leaf chemistry of clonal aspen (*Populus tremuloides*). *Journal of chemical ecology*, 32(7), pp.1415-1429. <https://doi.org/10.1007/s10886-006-9059-2>.
- Dührkop, K., Fleischauer, M., Ludwig, M., Aksenov, A.A., Melnik, A.V., Meusel, M., Dorrestein, P.C., Rousu, J. and Böcker, S., 2019. SIRIUS 4: Turning tandem mass spectra into metabolite structure information. *Nature Methods*, 16, 299–302 (2019).
<https://doi.org/10.1038/s41592-019-0344-8>.
- Dührkop, K., Nothias, L.F., Fleischauer, M., Reher, R., Ludwig, M., Hoffmann, M.A., Petras, D., Gerwick, W.H., Rousu, J., Dorrestein, P.C. and Böcker, S., 2021. Systematic classification of unknown metabolites using high-resolution fragmentation mass spectra. *Nature Biotechnology*, 39(4), pp.462-471. <https://doi.org/10.1038/s41587-020-0740-8>.
- Erwin, E. A., Turner, M. G., Lindroth, R. L., & Romme, W. H. (2001). Secondary Plant Compounds in Seedling and Mature Aspen (*Populus Tremuloides*) in Yellowstone National Park, Wyoming. *The American Midland Naturalist*, 145(2), 299–308.
<http://www.jstor.org/stable/3083108>.

- Evans JS, Oakleaf J, Cushman SA, Theobald D (2014) An ArcGIS Toolbox for Surface Gradient and Geomorphometric Modeling, version 2.0-0.
Available: <http://evansmurphy.wix.com/evansspatial>. (Accessed: 9/1/2020.)
- Hemming, J.D. and Lindroth, R.L., 2000. Effects of phenolic glycosides and protein on gypsy moth (Lepidoptera: Lymantriidae) and forest tent caterpillar (Lepidoptera: Lasiocampidae) performance and detoxication activities. *Environmental Entomology*, 29(6), pp.1108-1115. <https://doi.org/10.1603/0046-225X-29.6.1108>.
- Humphreys, N. 1996. Satin Moth in British Columbia. Natural Resources Canada, Canadian Forest Service, Pacific Forestry Centre, Victoria, BC. Forest Pest Leaflet 38. 4 p.
<https://d1ied5g1xfp8.cloudfront.net/pdfs/4610.pdf>. (Accessed: 11/1/2021)
- Lindroth, R.L. and Clair, S.B.S., 2013. Adaptations of quaking aspen (*Populus tremuloides* Michx.) for defense against herbivores. *Forest Ecology and Management*, 299, pp.14-21.
<https://doi.org/10.1016/j.foreco.2012.11.018>.
- Pellissier, L., Fiedler, K., Ndribe, C., Dubuis, A., Pradervand, J.N., Guisan, A. and Rasmann, S., 2012. Shifts in species richness, herbivore specialization, and plant resistance along elevation gradients. *Ecology and evolution*, 2(8), pp.1818-1825.
<https://doi.org/10.1002/ece3.296>.
- Rogers, P.C., Shepperd, W.D. and Bartos, D.L., 2007. Aspen in the Sierra Nevada: regional conservation of a continental species. *Natural Areas Journal*, 27(2), pp.183-193.
[https://doi.org/10.3375/0885-8608\(2007\)27\[183:AITSNR\]2.0.CO;2](https://doi.org/10.3375/0885-8608(2007)27[183:AITSNR]2.0.CO;2).
- Sardans, J., Gargallo-Garriga, A., Pérez-Trujillo, M., Parella, T.J., Seco, R., Filella, I. and Penuelas, J., 2014. Metabolic responses of *Quercus ilex* seedlings to wounding analysed with nuclear magnetic resonance profiling. *Plant Biology*, 16(2), pp.395-403.
- USDA Forest Service, Northern Research Station and Forest Health Protection. "Alien Forest Pest Explorer - species map." Database last updated 25 March 2019. (11/01/2021.)
- Wishart, D.S., Feunang, Y.D., Marcu, A., Guo, A.C., Liang, K., Vázquez-Fresno, R., Sajed, T., Johnson, D., Li, C., Karu, N. and Sayeeda, Z., 2018. HMDB 4.0: the human metabolome database for 2018. *Nucleic acids research*, 46(D1), pp.D608-D617.
<https://doi.org/10.1093/nar/gkx1089>.
- Wang, T., A. Hamann, D. Spittlehouse, and C. Carroll. 2016. Locally downscaled and spatially customizable climate data for historical and future periods for North America. *PLOS ONE* 11:e0156720. <https://doi.org/10.1371/journal.pone.0156720>.
- Young, B., Wagner, D., Doak, P. and Clausen, T., 2010. Within-plant distribution of phenolic glycosides and extrafloral nectaries in trembling aspen (*Populus tremuloides*; Salicaceae). *American journal of Botany*, 97(4), pp.601-610.
<https://doi.org/10.3732/ajb.0900281>.
- Ziemnicka, J., 2008. Outbreaks and natural viral epizootics of the satin moth *Leucoma salicis* L.(Lepidoptera: Lymantriidae). *Journal of Plant Protection Research*.
<https://doi.org/10.2478/v10045-008-0004-y>.

Appendix A: Supplementary material

Table 1: Seedling, sapling, and tree abundances by species in plots sampled across the Carson Range, NV/CA and in Dog Valley, CA. Means \pm 1 standard error are presented with the number of plots recording each species life stage.

	Seedlings (ha ⁻¹)	Saplings (ha ⁻¹)	Trees (ha ⁻¹)
Carson Range, NV/CA			
Quaking aspen (<i>Populus tremuloides</i>)	4783 \pm 553 (n=55)	3268 \pm 322 (n=54)	1211 \pm 87 (n=55)
Red fir (<i>Abies magnifica</i>)	418 \pm 99 (n=15)	159 \pm 45 (n=10)	88 \pm 23 (n=30)
White fir (<i>Abies concolor</i>)	418 \pm 99 (n=12)	114 \pm 48 (n=7)	94 \pm 32 (n=21)
Jeffery pine (<i>Pinus jeffreyi</i>)	279 \pm 145 (n=5)	70 \pm 12 (n=5)	58 \pm 19 (n=18)
Lodgepole pine (<i>Pinus contorta</i> var. <i>murrayana</i>)	149 \pm 0 (n=2)	87 \pm 24 (n=4)	37 \pm 9 (n=19)
Red alder (<i>Alnus tenuifolia</i>)	50 (n=1)	870 \pm 671 (n=2)	74 \pm 42 (n=7)
Western juniper (<i>Juniperus occidentalis</i>)	50 (n=1)	74 \pm 24 (n=2)	40 \pm 10 (n=3)
Western white pine (<i>Pinus monticola</i>)	0 (n=0)	50 (n=1)	10 \pm 10 (n=2)
Incense cedar (<i>Calocedrus decurrens</i>)	0 (n=0)	0 (n=0)	20 (n=1)
Dog Valley, CA			
Quaking aspen (<i>Populus tremuloides</i>)	1826 \pm 717 (n=7)	2338 \pm 786 (n=6)	1662 \pm 213 (n=7)
Red fir (<i>Abies magnifica</i>)	212 \pm 117 (n=4)	50 \pm 0 (n=2)	30 \pm 9 (n=6)
White fir (<i>Abies concolor</i>)	6018 (n=1)	0 (n=0)	25 \pm 10 (n=4)
Jeffery pine (<i>Pinus jeffreyi</i>)	896 \pm 845 (n=2)	149 \pm 50 (n=2)	113 \pm 47 (n=5)
Incense cedar (<i>Calocedrus decurrens</i>)	2114 \pm 1964 (n=2)	50 (n=1)	76 \pm 65 (n=2)

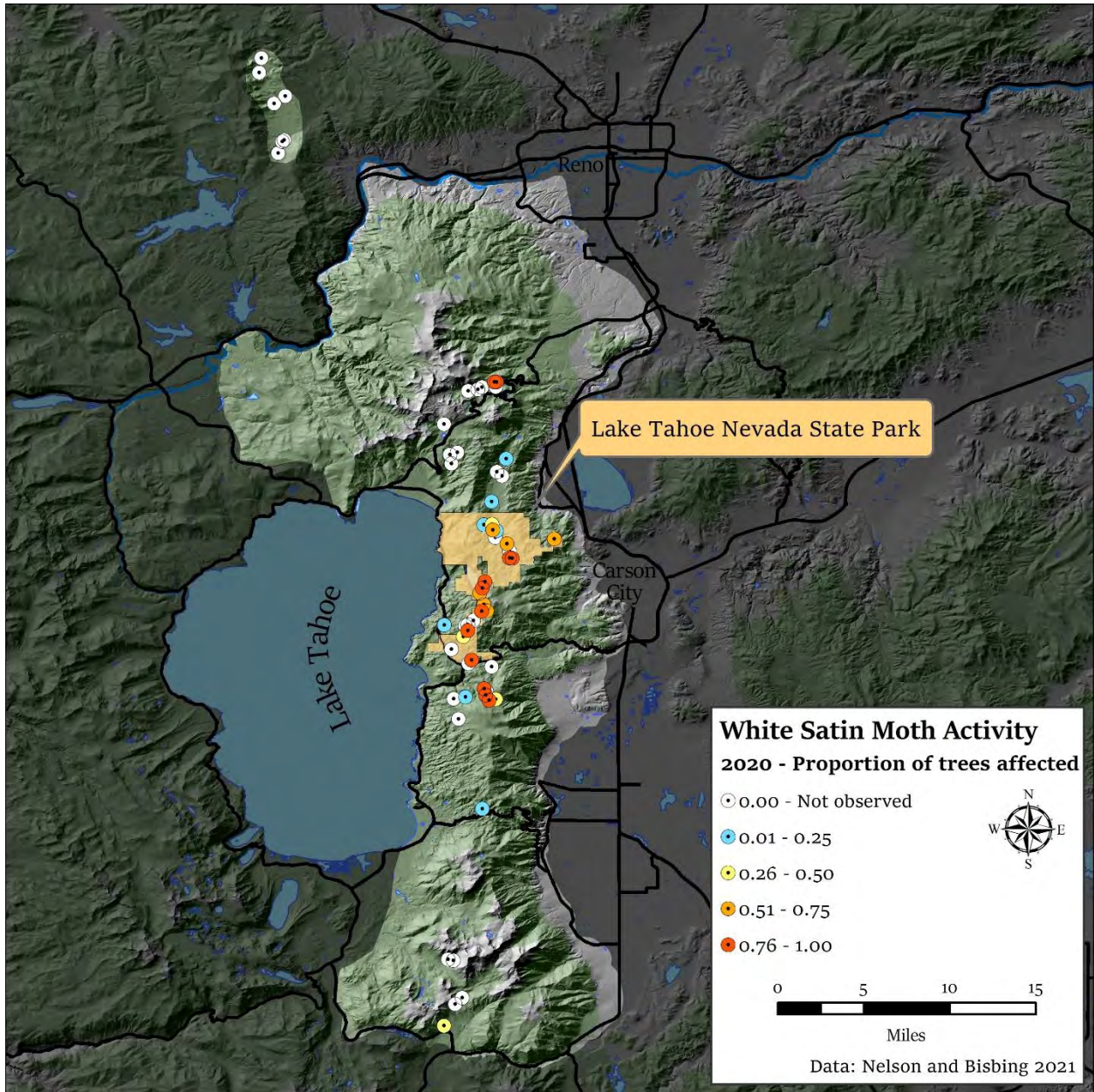


Figure 1: White satin moth occurrence and proportion of trees affected by white satin moth in plots sampled across the Carson Range, NV/CA and Dog Valley, CA